Spin Flop Transition in a Finite Antiferromagnetic Superlattice: Evolution of the Magnetic Structure

S. G. E. te Velthuis, J. S. Jiang, S. D. Bader, and G. P. Felcher

Materials Science Division, Argonne National Laboratory, 9700 South Cass Avenue, Argonne, Illinois 60439

(Received 7 May 2002; published 3 September 2002)

An antiferromagnetic (AF) superlattice of Fe/Cr(211) is used as a model system to study magnetic transitions in a finite-size geometry. With polarization neutron reflectometry the magnetic structure at the surface spin-flop transition and its evolution with field is determined. A domain wall created near the surface penetrates the superlattice with increasing field, splitting it into two antiphase, AF domains. After reaching the center the spin-flopped phase spreads throughout the superlattice. The experimental results are in substantial agreement with theoretical and numerical predictions.

DOI: 10.1103/PhysRevLett.89.127203 PACS numbers: 75.70.–i, 61.12.Ha, 75.25.+z, 75.50.Ee

Uniaxial antiferromagnets (AFs) have occupied the attention of researchers since Néel first predicted [1] the magnetic field conditions under which an AF exhibits a spin-flop transition, which is an abrupt decoupling between the direction of the AF and the easy axis (EA). In Néel's microscopic description, below a critical field the magnetic moments are ordered in two sublattices with opposite magnetization **M**. Their orientation is along the EA, as is the applied field **H**, but at the bulk spin-flop transition $H^B_{\rm SF}$ the sublattice **M** is canted with a resulting net M along **H**. Interestingly, it took over 30 years before experiments confirmed Néel's model [2].

AF coupled metallic superlattices (SL) offer novel templates to study the behavior of magnetic structures in reduced dimensionality, in our case a finite AF. The two outer layers (facing the surface and the buffer/substrate) are each magnetically coupled on only one side, and they respond more readily to an external field. In 1968 Mills proposed [3] that in an AF with a free surface, spins near the surface rotate into a flopped state at a field smaller than $H^B_{\rm SF}$. Later Keffer and Chow [4] refined the description of the surface spin-flop (SSF). To describe the behavior of bulk and finite antiferromagnets the important quantities are the exchange field H_E and the anisotropy field H_A. The descriptions discussed here are limited to systems for which H_E and H_A are of the same order of magnitude [5]. For a finite system composed of an even number of AF coupled layers, a SSF transition takes place at $(H^S_{\rm SF})^2 = H_E H_A + H_A^2$ and the bulk spin-flop field occurs at $(H^B_{\rm SF})^2 = 2H_E H_A + H_A^2$. $H_A = 2K_u/M_s$, where K_u is the uniaxial anisotropy and M_s is the saturation magnetization, while $H_E = 2J/M_s t$, where J is the exchange coupling and $M_s t$ is the moment per surface area [6]. Keffer and Chow pointed out that, with increasing H, the SSF must penetrate the superlattice (SL) as an AF domain wall, until it reaches the center of the stack. Then the spin-flopped region should expand to the full extent of the SL.

In 1994 magnetic measurements by Wang *et al.* [7] on Fe/Cr(211) superlattices confirmed the presence of a SSF transition. The SL was chosen with a Cr layer thickness that gives AF coupling of adjacent Fe layers, and was grown epitaxially on a MgO(110) substrate to provide uniaxial magnetic anisotropy [6]. Application of **H** parallel to the in-plane EA indeed initiated a magnetic transition at a field lower than $H^B_{\rm SF}$. The surface character of this transition was identified by magneto-optical Kerr effect (MOKE) measurements. MOKE is surface sensitive since the depth penetration of the laser light is less than the film thickness, When the surface layer was magnetized opposite to **H** it was not detected because it nucleated at the buried surface. In contrast, magnetometry, probing the entire sample volume, detected the surface spin-flop transition in both field directions.

Following the experiments by Wang *et al.* in 1994 [7], a robust body of theoretical and computational work amassed to describe in detail the microscopic underpinning of this behavior [8–12]. The region of flopped spins, created at one end of the SL at $H^S_{\rm SF}$, is described as moving toward its center by jumps. The transition progresses with increasing H by a pair of layers of the inner domain becoming part of the outer domain (whose **M** is along **H**). There is "discommensuration" [11]: the moving wall separates the SL into two domains, with magnetizations symmetric to the wall [9] or, as said in crystallography, in antiphase. Also its spreading toward the edges of the SL occurs by a series of discrete jumps [10]. The process is completed at $H^B_{\rm SF}$. A visualization of the field evolution of the magnetic structure is presented in Fig. 1. Each compass represents **M** of an Fe layer in the SL stack. **H** is the direction of the applied field, along the AF easy axis in the film plane. The fields are scaled with respect to the bulk spin-flop field ($h = H/H^B_{\rm SF}$). The object of the present Letter is to show that, on the basis of polarized neutron reflectivity (PNR) measurements, the description given above is correct to a remarkable degree. Figure 1 actually has not been obtained by numerical calculations [8–10], but is the result of a least square fitting of the neutron data.

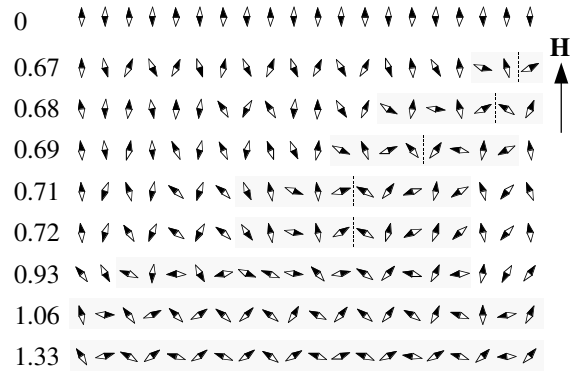

FIG. 1. The compasses in each row depict the magnetization direction in the Fe layers across the SL stack at increasing applied fields, starting with the AF alignment at zero field. The applied field $h\,(=H/H^B_{\rm SF})$ is given to the left of each row. The gray shading indicates approximately the area of the domain wall, while the vertical dashed line indicates the position of the discommensuration that divides the system into two domains in antiphase. The directions of the moments as shown are obtained by fitting the PNR data in Fig. 3.

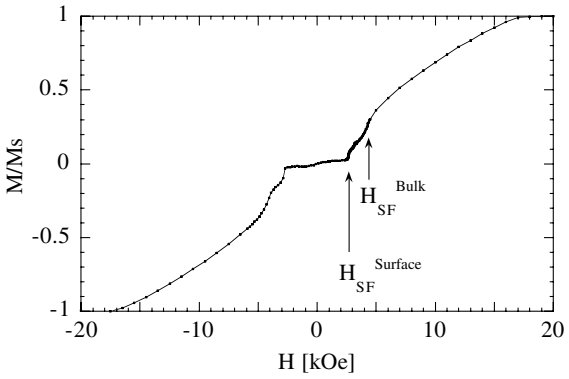

FIG. 2. Magnetization curve of the $[\mathrm{Fe}(14\ \text{Å})/\mathrm{Cr}(11\ \text{Å})]_{20}$ superlattice.

We studied the spin-flop transition of an AF coupled Fe/Cr SL of the type $[\mathrm{Fe}(14\ \text{Å})/\mathrm{Cr}(11\ \text{Å})]_{20}$. The thickness appears within parentheses and there are 20 repeats of Fe/Cr bilayers. The sample was prepared via dc magnetron sputtering onto a single-crystal MgO(110) substrate. A Cr buffer layer, nominally 200-Å thick, was first deposited at 400 °C to establish epitaxy with the substrate. The SL was deposited at 100 °C and found to grow with a (211) orientation [6]. The SL was capped by a 100-Å Cr layer. The epitaxy and the perfection of the SL were checked by x-ray diffraction. In particular, low angle x-ray reflectivity measurements indicate an Fe/Cr interfacial roughness of 4 Å. Magnetically the sample was characterized by SQUID magnetometry as well as by MOKE, with **H** along the EA, in the plane of the film. In SQUID measurements (Fig. 2) the induced M is interpreted as the onset of the SSF ($H^S_{\rm SF}$). Further increasing H, the magnetic susceptibility steadily increases until 4.14 kOe, indicating that at this field the entire SL has undergone a spin-flop ($H^B_{\rm SF}$). Saturation is reached at 16.7 kOe, with $M_s t \approx 1.8 \times 10^{-4}$ emu/cm^2 per Fe layer. The experimental phase transitions and M fit well with the values expected for superlattices, for which $K_s \sim 0.06$ erg/cm^2 [5] giving $J_{\rm AF} \sim 0.81$ ergs/cm^2, $H^S_{\rm SF} = 3.3$ kOe, and $H^B_{\rm SF} = 4.4$ kOe.

PNR measurements were carried out at the "POSY I" reflectometer at the Intense Pulsed Neuron Source of Argonne National Laboratory [13]. The sample, of $\sim$4 cm^2 area was inserted in the gap of a conventional, split-coil electromagnet, with a maximum field of 6 kOe and with a field homogeneity of 5% on the sample. The quantities measured as a function of the neutron momentum transfer perpendicular to the surface, $q \equiv 4\pi \sin\theta/\lambda$ (θ angle of incidence, λ wavelength of the neutron), are the reflectivities: R^{++}, R^{+-}, R^{-+}, and R^{--}, where the two superscripts denote the orientation of the polarization, parallel (+) or opposite (−) to **H**, before and after reflection from the sample, respectively. From R a chemical and magnetic depth profile from the surface to the substrate can be determined [14]. Specifically, R^{+-} and R^{-+} are solely due to the components of **M** perpendicular to **H**. All four measured reflectivities were corrected for polarization efficiency.

Initial PNR experiments indicated that at $H \approx 0$, after saturation in ± 50 kOe, the sample consists of lateral domains. This is given by the fact that the two non-spin flip reflectivities, R^{++} and R^{--}, are equal. The lateral domains are AF ordered throughout the thickness of the SL, but the top layer is either parallel or perpendicular to the priming field. If the lateral domains had been of the order of a few μm or less, off-specular scattering would have been observed [15]. Since this was not the case, the domains can be assumed to be significantly larger. Only after cycling within the minor loop ($\pm$ 6 kOe), a majority of one domain state was formed, evidenced by a difference in R^{++} and R^{--}. The measurements of the spin-flop transition presented here were performed after cycling within the minor loop and with a final "priming" field of +6 kOe.

As a result of the periodic chemical and magnetic structure of the sample, the PNR spectra include Bragg reflections which have maxima at $q = 2\pi/d$, where d is the period of the structure. The first Bragg reflection that appears at low q is an AF peak. In Fig. 3, R^{++}, R^{--}, and R^{-+} are presented for ascending values of h ($= H/H^B_{\rm SF}$, with $H^B_{\rm SF} = 4.14$ kOe). The $h = 0$ spectra are consistent with that of an AF alignment, with the magnetization of the top Fe layer opposite to **H**. As $h > h^S_{\rm SF} \approx 0.66$, the intensity and width of the Bragg peak (at $q = 0.131$ Å^{-1}) change. For R^{++} and R^{--}, the peak broadens and eventually seems to split into two parts (i.e., a minimum is created at the center). Correlated with this is the growth and sharpening of the Bragg peak in the spin flip reflectivity R^{-+}.

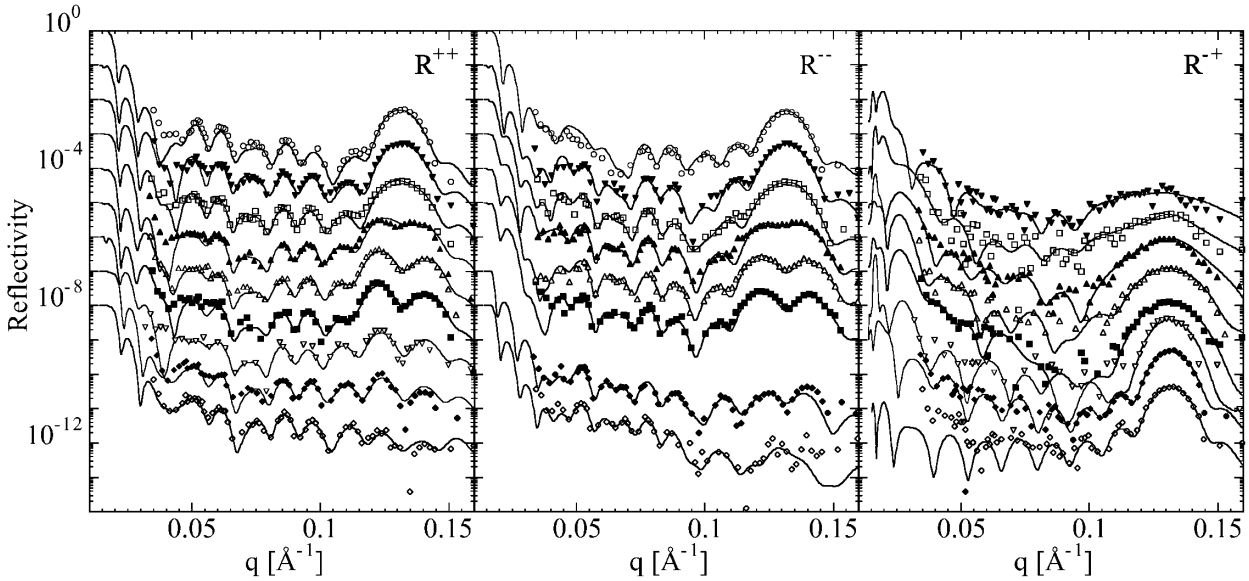

FIG. 3. The evolution of R^{++}, R^{--}, and R^{-+} as a function of increasing h (going from the top to the bottom curve), the values of which are the same as those in Fig. 1. Symbols represent the data, while the solid lines are fitted to the data. For clarity, data at sequential fields are displaced by a decade downwards.

Basic crystallography can explain these observations. Within the first Born approximation, a periodic array of $2N$ equal scattering objects, each of scattering amplitude a and of thickness d, gives rise to a Bragg reflection with intensity [16]:

$$I_0 \propto a^2\{\sin[qd(2N)/2]/\sin[qd/2]\}^2, \quad (1)$$

which at its maximum at $q = 2\pi/d$, is proportional to $(2N)^2$. The distance between the first two minima and that value is $\Delta q_m = \pm[1/(2N)]2\pi/d$, which depends on the number of scattering objects $2N$. When a displacement of length $d/2$ is introduced in the center of the array, the array is divided into two equal domains in antiphase. The diffracted intensity then becomes

$$I_a \propto a^2\{\sin[qd(N)/2]/\sin[qd/2]\}^2 \times \cos^2\{qd[(N)/2 + 1/4]\}, \quad (2)$$

which has a minimum at $q = 2\pi/d$ splitting the Bragg reflection. Now $\Delta q_m \approx \pm[1/N]2\pi/d$.

In our case the "scattering object" consists of a pair of adjacent Fe layers with opposite **M**, i.e., one period of the AF structure. At least for values of q far exceeding the edge of total reflection, R^{++} and R^{--} are due to the component of **M** along **H**. The splitting of the Bragg peak observed for R^{++} and R^{--} above $h = 0.69$ is due to the formation of two domains where the components of **M** collinear to **H** are in antiphase. In the case in which the two domains have different thicknesses, the intensity close to $q = 2\pi/d$ has a smoother variation. However, the Δq_m of the auxiliary minima is dictated by the largest of the two domains. R^{+-} and R^{-+} are nonzero only when there are components of **M** perpendicular to **H**. The shape of the Bragg peak in R^{-+} is given by Eq. (1). The size of the flopped region, i.e., the extension of the domain wall, can be determined from the relevant Δq_m around the Bragg peak position. These considerations show how to extract in a straightforward way, by approximation, the position and width of the domain wall, from the reflectivities of Fig. 3. The results are shown in Fig. 4. In agreement with results of numerical calculations, the domain wall reaches the center of the SL when $h\text{-}h^S_{\mathrm{SF}} = 0.08$.

More detailed magnetic depth profiles were obtained by fitting the full set of measured spin-dependent reflectivities using a least square minimization procedure [17]. Data taken at $h = 0$ were used to fit the chemical depth profile, i.e., the layer thickness and roughness, with the

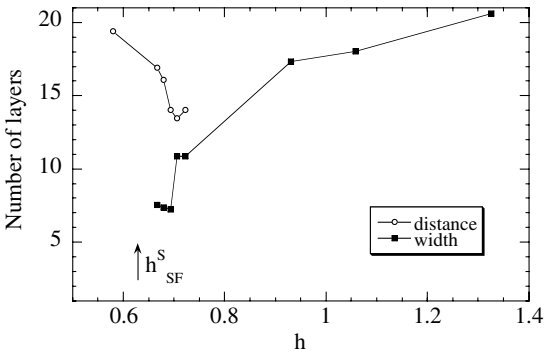

FIG. 4. Distance of the domain wall from the bottom layer, as obtained from the position of the auxiliary minima around the AF reflection (R^{++} data). Width of the domain wall, in number of layers that are spin-flopped (R^{-+} data).

assumption that the magnetic configuration is AF and along **H**. Subsequently, for higher h, the orientation of **M** of each of the 20 Fe layers was fitted. M is an additional fitting parameter, but it has one value for all 20 layers. The fitted reflectivities are the solid lines in Fig. 3, while the results for the direction of the layer-by-layer magnetizations are displayed in Fig. 1. The results confirm that the spin-flop transition initially starts at the top surface, forms a domain wall, and propagates to the center. The region of fields where the wall is expected to widen was not well covered by the measurements. Yet at $h = 0.93$ there is almost a completely formed spin-flopped state. At the two highest fields, the moments are canted towards **H**. The fitting routine gives the error in the determined directions of **M** to be $\sim 5°$ on average. However, taking into account the uniqueness of the solution, we estimate that the real error is $\sim 20°$. Still, the magnetic evolution illustrated in Fig. 1 is strikingly similar to that calculated [8,9]. To attain the magnetic structure at each field with greater precision, it would be beneficial to calculate the reflectivity expected from the computed magnetic structures (which unfortunately so far have been reported in the literature only in graphical, rather than numerical form).

Still remaining to be experimentally verified are the discontinuities as the domain wall propagates toward the center and spreads throughout the entire SL [8–12]. These transitions should be observable as spikes in the magnetic susceptibility with changing H—but have not yet been observed. Furthermore, PNR measurements so far do not support a proposition [9] that the antiphase state is metastable when H is lowered well below H_{SF}^{S}. This state was never observed at $H \approx 0$, not after saturating at 50 kOe, nor after cycling the minor loop up to 6 kOe.

The spin-flop transition in a finite system has been discussed for the case that **H** is applied along the EA. For a bulk AF, the phase diagram as a function of the tilt angle α from the EA is well known. In two dimensions [18,19] the spin-flop transition remains first order when α is smaller than a critical value α_c, which can be a fraction of a degree. The highest field at which the AF structure is stable, and the lowest field at which the spin-flop state is stable, continue to approach each other with increasing α, until they join at $\alpha_c = H_E/(2H_E + H_A)$. At this point the magnetization vectors of the two sublattices form an angle of 90°. For larger values of α, the rotation of magnetic moments with field is continuous. In order to ensure that **H** was parallel to the EA in our experiments, we performed MOKE measurements as a function of α within the film plane. The character of the EA transition was preserved within the angular range $\alpha_c = \pm 6^{\circ}$. Beyond this boundary other first-order transitions occurred whose nature is as yet unexplained. It is our hope that an expansion of the theories so far developed for the spin-flop transition in finite systems will provide guidance to further experiments.

In conclusion, with PNR measurements we have successfully determined the layer-by-layer magnetization profile in a finite, uniaxial AF at different stages of the surface and bulk spin-flop transitions. Our results show that the surface transition follows the general trend that had been predicted, in particular, that the motion of the spin-flopped region toward the center of the SL results in two antiphase domains.

This work was supported by the U.S. DOE, Office of Science under Contract No. W-31-109-ENG-38. The authors thank J. Meersschaut, A. Hoffmann, C. Micheletti, and A. Rettori for useful discussions. After completing this work we received a preprint (Lauter-Pasyuk *et al.* [20]) in which the splitting of the AF Bragg peak indicating the antiphase domain in a SL of Fe/Cr(100) was also observed.

[1] L. Néel, Ann. Phys. (Paris) **5**, 232 (1936).
[2] For a review, see Y. Shapira and S. Foner, Phys. Rev. B **1**, 3083 (1970).
[3] D. L. Mills and W. M. Saslow, Phys. Rev. **171**, 488 (1968).
[4] F. Keffer and H. Chow, Phys. Rev. Lett. **31**, 1061 (1973).
[5] L. Trallori *et al.*, J. Phys. Condens. Matter **7**, L451 (1995).
[6] E. E. Fullerton *et al.*, Phys. Rev. B **48**, 15 755 (1993).
[7] R. W. Wang *et al.*, Phys. Rev. Lett. **72**, 920 (1994).
[8] S. Rakhmanova, D. L. Mills, and E. E. Fullerton, Phys. Rev. B **57**, 476 (1998).
[9] N. Papanicolaou, J. Phys. Condens. Matter **10**, L131 (1998); **11**, 59 (1999).
[10] L. Trallori, Phys. Rev. B **57**, 5923 (1998).
[11] C. Micheletti, R. B. Griffiths, and J. M. Yeomans, J. Phys. A **30**, L233 (1997); Phys. Rev. B **59**, 6239 (1999).
[12] A. L. Dantas and A. S. Carriço, Phys. Rev. B **59**, 1223 (1999).
[13] G. P. Felcher *et al.*, Rev. Sci. Instrum. **58**, 609 (1987); T. Krist, F. Klose, and G. P. Felcher, Physica (Amsterdam) **248B**, 372 (1998).
[14] J. F. Ankner and G. P. Felcher, J. Magn. Magn. Mater. **200**, 741 (1999).
[15] G. P. Felcher and S. G. E. te Velthuis, Appl. Surf. Sci. **182**, 209 (2001).
[16] R. W. James, *The Optical Principles of the Diffraction of X-Rays* (Ox Bow Press, Woodbridge, Connecticut, 1962).
[17] R. W. E. van de Kruijs *et al.*, Phys. Rev. B **65**, 064440 (2002).
[18] H. Rohrer and H. Thomas, J. Appl. Phys. **40**, 1025 (1969).
[19] J. M. Kosterlitz, D. R. Nelson, and M. E. Fisher, Phys. Rev. B **13**, 412 (1974).
[20] V. Lauter-Pasyuk *et al.* (unpublished).